# Effect of process conditions on the growth of radio-frequency sputtered amorphous carbon films

D. Wan and K. Komvopoulos

*Department of Mechanical Engineering, University of California, Berkeley, CA 94720*

**Abstract**

Amorphous carbon (a-C) films were synthesized by low-pressure radio-frequency (rf) discharge in pure Ar atmosphere, and the effect of plasma conditions on the growth of sputtered a-C films were investigated experimentally by transmission electron microscope (TEM) and atomic force microscope (AFM). It was found that the sputtered a-C film thickness was linearly dependent on the product of the sputtering rate and deposition time. The principal factors affecting the film surface roughness were the film growth rate and the intensity of the $Ar^+$ bombardment. In the absence of $Ar^+$ bombardment, the faster film growth the rougher the film surface. However, in the presence of $Ar^+$ bombardment on the growing film surface, the a-C film surface roughness was controlled by the intensity of the bombardment. The film surface roughness was improved (rms surface roughness < 0.2 nm) with increasing $Ar^+$ kinetic energy up to ~ 200 eV. However, for $Ar^+$ bombardment energy above ~210 eV, the surface roughness increased due to the combined effects of increases resputtering and, especially, high irradiation damage.

## I. INTRODUCTION

Hydrogen-free amorphous carbon (*a-C*) films deposited by various methods exhibit excellent physical properties (Tsai et al., 1987; Lifshitz, 1997; Robertson, 2002). Formation of ultrathin carbon films on a highly oriented pyrolytic graphite substrate has been accomplished by the deposition of low-energy carbon ions at temperatures from ambient to 300$^{o}$C (Durand et al., 1998). Roughening due to the transition from lateral island growth to three-dimensional film growth was found to depend on the substrate temperature and ion-current density. The surface roughness, density, percentage of $sp^3$ tetrahedral carbon bonding, and internal compressive stresses of ultrathin *a*-C films deposited by sputtering under a positive substrate bias voltage decreased with the increase of the film thickness (Logothetidis et al., 1997). Applying a negative bias voltage to the substrate during sputter deposition in a pure Ar atmosphere was reported to significantly increase the density as a result of the transition from trigonal ($sp^2$) to tetragonal ($sp^3$) carbon hybridizations under high compressive stress (Schwan et al., 1997). Intense energetic particle bombardment on a growing *a*-C film surface strongly affects the compressive stress level; however, the relationship between the intense bombardment and the produced compressive stress level appears to be complex (Windischmann, 1992; Davis, 1993).

During rf sputter deposition under low working pressure (~3 mTorr), collisionless plasma sheaths are produced which increase the ion impinging fluxes on both target and substrate surfaces. The absorbed rf power directly influences the ion density in the plasma bulk and the ion fluxes at the plasma sheath edges. The kinetic energy of the ions bombarding the growing film surface depends on the substrate bias voltage and influences the ion bombardment effect. In this study, the effect of low-pressure Ar rf discharge on the growth of ultrathin *a-C* films synthesized by rf sputter deposition was investigated experimentally, and the roles of the above factors were analyzed in light of experimental results obtained from sputtered *a*-C films.

## II EXPERIMENTAL PROCEDURES

Ultrathin *a-C* films were deposited on Si(100) substrates by $Ar^+$ sputtering of a pure graphite target using a Perkin-Elmer Randex-2400 model sputtering system without magnetron. The vacuum chamber was first pumped down to a low base pressure (< $2\times10^{-6}$ Torr) to reduce the effect of residual gases before introducing the Ar gas into the process chamber. Before film deposition, the graphite target was sputter cleaned for 3-20 min, depending on the previous time of exposure of the chamber to the atmosphere, and the Si(100) substrate was sputter etched for 3 min to remove a surface layer of thickness ~40 nm. The precleaning process was carried out at 250 W forward rf power, 3 mTorr working pressure, and 20 sccm argon gas flow rate.

Ultrathin *a-C* films were synthesized under conditions of forward rf power in the range of 200-750 W, substrate bias voltage between 0 and -500 V, working pressure of 3 mTorr, gas flow rate of 20 sccm, and deposition time in the range of 3-11 min. Film surface roughness measurements were obtained from 1 $\mu m^2$ surface area images obtained with an AFM (Digital Instruments, NanoScope II), and the root-mean-square (rms) surface roughness was calculated as the average of five rms values obtained from different surface area images of the same film sample. The film thickness was measured directly from cross-sectional images taken at different positions of the same sample using a high-resolution TEM (Philip CM300FEG/UT).

## III RESULTS AND DISCUSSION

### A. Ar ion impinging flux and Ar-ion-induced sputtering yield of graphite

Figure 1 shows schematically the processes of *a*-C film deposition by $Ar^+$ sputtering involving three sequential processes: (i) sputtering of carbon atoms from graphite target by energetic $Ar^+$, (ii) carbon atom transport through the plasma space between the target and the substrate, and, (iii) surface diffusion of arriving carbon atoms on the substrate to form stable chemical bonds with other carbon atoms. The growth rate of the *a-C* film depends on the carbon atom flux at the substrate, carbon atom resputtering rate from the film surface, and carbon atom redeposition from the residual carbon layer deposited on the substrate holder (Figure 1). However, the later effect can be neglected because the surface area of the Si(100) substrate is much smaller than that of the substrate holder and the moving directions of resputtered carbon atoms from the residual carbon layer are random. The flux of the carbon atoms at the substrate is directly related to the $Ar^+$ impinging flux $J_{Ar^+}$ and sputtering yield of carbon $\gamma$, which is defined as the number of carbon atoms ejected from the bombarded target per incident energetic $Ar^+$.

Based on energy balance consideration, the $Ar^+$ impinging flux $J_{Ar^+}$ can be expressed as

$$J_{Ar^+} = \frac{P_a}{eA(2V_p - V_T - V_S)}, \tag{1}$$

where $e$ is the electron charge. $J_{Ar^+}$ increases with the absorbed rf power $P_a$ when the working pressure is maintained constant.

Sputtering of the target by energetic $Ar^+$ is essentially a process involving cascades of atomic collisions. Sigmund (1969) proposed a theory to calculate the sputtering yield of amorphous and polycrystalline materials based on the assumption of random slowing down of the ions in an infinite medium. The sputtering yield of a solid is a function of the energy of the incident ions. Matsunami et al. (1984) compiled the available experimental data graphically, and developed an empirical formula of the energy dependent ion-induced sputtering yields of monatomic solids for various ion-target combinations, given by:

$$\gamma = 0.42 \frac{\alpha^* Q K s_n(\varepsilon)}{U_s[1 + 0.35 U_s s_e(\varepsilon)]}[1 - (\frac{E_{th}}{E})^{1/2}]^{2.8}, \quad (2)$$

where $\alpha^*$, $Q$, $E_{th}$ are empirical parameters, $U_s$ is the target sublimation energy (eV), $E$ is the energy of incident ions, $s_n$ and $s_e$ are Lindhard's elastic and inelastic reduced stopping cross sections, respectively, and $\varepsilon$ is the reduced energy. For graphite target, $Q$=3.1 ± 0.9 and $U_s$=7.37 eV. The express for the reduced energy is (Matsunami et al., 1984):

$$\varepsilon = \frac{0.03255}{Z_1 Z_2 (Z_1^{2/3} + Z_2^{2/3})^{1/2}} \frac{M_2}{M_1 + M_2} E \text{ (eV)}. \quad (3)$$

The elastic and inelastic reduced stopping cross sections are given by (Matsunami et al., 1984):

$$s_n = \frac{3.44\sqrt{\varepsilon}\ln(\varepsilon + 2.718)}{1 + 6.355\sqrt{\varepsilon} + \varepsilon(-1.708 + 6.882\sqrt{\varepsilon})}, \quad (4)$$

and

$$s_e = 0.079 \frac{(M_1 + M_2)^{3/2}}{M_1^{3/2} M_2^{1/2}} \frac{Z_1^{2/3} Z_2^{1/2}}{(Z_1^{2/3} + Z_2^{2/3})^{3/4}} \sqrt{\varepsilon}. \quad (5)$$

In Eqs. (3) - (5), $Z_1$ and $Z_2$ are the atomic numbers of the incident ions and target atoms, and $M_1$ and $M_2$ are their mass numbers, respectively. The empirical parameter $\alpha^*$ is expressed as (Matsunami et al., 1984):

$$\alpha^* = 0.08 + 0.164(\frac{M_2}{M_1})^{0.4} + 0.0145(\frac{M_2}{M_1})^{1.29}. \quad (6)$$

The empirical parameter $E_{th}$ is given by (Matsunami et al., 1984):

$$\frac{E_{th}}{U_s} = 1.9 + 3.8(\frac{M_2}{M_1})^{-1} + 0.134(\frac{M_2}{M_1})^{1.24}, \quad (7)$$

under the condition of $Ks_n(\varepsilon) > 2.5$ eV-cm$^2$/10$^{15}$ atoms to avoid the influence of nonlinear effect on the empirical parameters, where $K$ is the conversion factor in units of eV-cm$^2$/10$^{15}$ atoms defined as (Matsunami et al., 1984):

$$K = \frac{S_n}{s_n} = 8.478 \frac{Z_1 Z_2}{(Z_1^{2/3} + Z_2^{2/3})^{1/2}} \frac{M_1}{M_1 + M_2} . \tag{8}$$

The sputtering yields of the graphite target were calculated using the above equations under different $Ar^+$ bombarding conditions. Figure 2 shows that the sputtering yield $\gamma$ and $Ar^+$ impinging flux $J_{Ar^+}$ increase with the forward rf power for substrate bias voltage $V_S$ and working pressure fixed at –200 V and 3 mTorr, respectively. Figure 3 shows that the sputtering yield $\gamma$ decreases with the increase of the negative substrate bias voltage for forward rf power and working pressure maintained at 750 W and 3 mTorr, respectively. However, the impinging flux $J_{Ar^+}$ is nearly independent of the substrate bias voltage.

### B. Effect of process conditions on the growth of *a*-C films

The effect of process conditions in low-pressure Ar rf discharge on the growth of *a*-C films was investigated experimentally at working pressure of 3 mTorr and gas flow rate of 20 sccm. All the results are given in Tables 1 through 3. Table 1 shows the effect of absorbed rf power $P_a$ on the *a*-C film thickness and roughness for substrate bias voltage of -200 V and 0 V and deposition time of 3min. The absorbed rf power $P_a$ varied in the range of 170-742 W. Table 2 shows the effect of substrate bias voltage $V_S$ varied between 0 and -500 V on the *a*-C film thickness and roughness for forward rf power equal to 750 W and deposition time equal to 3 min. Table 3 shows the effect of deposition time varied from 3 to 11 min on the *a*-C film thickness for forward rf power of 750 W and substrate bias voltage of -200 V. All of the film thickness data listed in the above tables were obtained directly from high-resolution cross-sectional TEM images. Figure 4 shows a TEM image of an *a*-C film deposited under forward rf power of 750 W, substrate bias voltage of –200 V, working pressure of 3 mTorr, gas flow rate 0f 20 sccm and deposition time of 3 min.

As discussed previously, the *a*-C film thickness depends on the number of carbon atoms arriving at the substrate surface and the number of resputtered carbon atoms removed from the surface. There are two competing factors that determine the number of carbon atoms arriving at the substrate surface: the sputtering rate $\beta$, defined as the number of atoms sputtered off from a unit area of the target surface per unit time, and the scattering effect of carbon atoms during transport through the target-substrate plasma space. The sputtering rate $\beta$ is a product of the sputtering yield $\gamma$ and $Ar^+$ impinging flux $J_{Ar^+}$,

$$\beta = \gamma J_{Ar^+} . \tag{9}$$

The scattering effect is inversely proportional to $\lambda / L$, where $L$ is the distance between the target and the substrate, and $\lambda$ is the mean free path of the particles given by

$$\lambda = \frac{k_B T}{\sqrt{2}\pi d^2 p}, \tag{10}$$

where $T$ is the bulk plasma temperature, which is significantly higher than the room temperature (300 K) (Lieberman et al., 1994), *d* is the particle diameter (< 3 Å), and *p* is the working pressure. The target-substrate distance $L$ in the present sputtering system is fixed at 7 cm. For $p$=3 mTorr (0.4 Pa), the mean free path $\lambda$ of the particles is larger than 10 cm. Therefore, $\lambda / L$ >1 and the scattering effect on the film growth is marginal in the present experiments.

The number of resputtered carbon atoms from the growing film surface depends on the intensity of the $Ar^+$ bombardment. Assuming that the $Ar^+$ induced sputtering yield of the *a*-C film surface is equal to the $Ar^+$ induced sputtering yield of the graphite, the sputtering yield $\gamma_S$ of the *a*-C film due to $Ar^+$ bombardment can be determined from Eq. (2). The relationship between ratio $\gamma/\gamma_S$ and absorbed rf power $P_a$ for the substrate bias voltage equal to -200 V is shown in Figure 5. The ratio $\gamma/\gamma_S$ is less than 10% for the absorbed rf power $P_a$ larger than 200 W. Hence, the resputtering effect due to $Ar^+$ bombardment on the growing *a*-C film surface is secondary in film growth.

In view of the aforementioned, it may be concluded that the *a*-C film thickness $t_f$ depends mainly on the sputtering rate $\beta$ and deposition time $t$ for fixed room temperature deposition, i.e.,

$$t_f \propto t\beta . \qquad (11)$$

Figure 6 shows the relationship between the measured film thickness data and the product of the sputtering rate $\beta$ and deposition time $t$. This linear relationship result is excellent agreement with the above interpretation (Eq. (11)).

### C. Effect of process conditions on *a*-C Film surface roughness

$Ar^+$ bombardment exhibited a significant effect on the *a*-C film surface roughness. Figure 7 shows the effect of the substrate bias voltage on the *a*-C film surface roughness. The films were deposited at room temperature in a pure Ar plasma atmosphere under conditions of forward rf power of 750 W, working pressure of 3 mTorr, gas flow rate of 20 sccm, and deposition time of 3 min. In the absence of substrate bias voltage, film growth was mainly controlled by the flux of impinging carbon atoms, surface temperature, and surface diffusion. At room temperature deposition, the previous deposition conditions leaded to a relatively high content of trigonal carbon bonding ($sp^2$) and rough surface topography (typical rms surface roughness was ~1.13 nm). Applying a negative bias voltage to the substrate promoted $Ar^+$ bombardment on the growing film surface, which promoted random surface motion of the carbon atoms. This effect enhanced more carbon atoms to form strong tetrahedral bonds ($sp^3$) and produced a smooth surface. The smoothest *a*-C films were deposited under substrate bias voltage of –200 V. These film exhibited an rms roughness of only ~0.12 nm. At relatively high bias voltages (i.e., intensive $Ar^+$ bombardment), irradiation damage and roughening of the film surface occured due to intensification of the resputtering and $Ar^+$ implantation effects.

The effect of the forward rf power on the film surface roughness was also investigated by depositing *a*-C films under conditions of working pressure of 3 mTorr, gas flow rate of 20 sccm, deposition time of 3 min, and varied forward rf power. In the presence of $Ar^+$ bombardment during film deposition due to substrate bias voltage of -200 V, the surface rms roughness varied in a narrow range for forward rf power between 250 and 750 W (Figure 8). Hence, the effect of the forward rf power on the film surface roughness was secondary because the random motions of the carbon atoms at the growing film surface were controlled by the $Ar^+$ bombardment. However, the film surface roughness was strongly affected by the forward rf power in the absence of $Ar^+$ bombardment during film deposition (zero substrate bias) (Figure 8). The rms roughness increased from 0.32 nm to 1.13 nm as the forward rf power increased from 300 to 750 W. The increase of the forward rf power in this range resulted in the increase of both the $Ar^+$ impinging flux and film growth rate from $5.16 \times 10^{15}$ to $8.08 \times 10^{15}$ ions/s·cm$^2$ (Table 1) and 0.81 to 1.89 Å/s, respectively. The increase of the density of carbon atoms arriving at the film surface prevented the surface diffusion of carbon atoms, producing a thick and rough *a*-C film. Therefore, in the absence of $Ar^+$ bombardment, the film growth rate exhibited significant correlation with the *a*-C film surface roughness.

The effect of the Ar gas flow rate was investigated for conditions of forward rf power of 750 W, substrate bias voltage of –200 V, working pressure of 3 mTorr, and deposition time of 3 min. Figure 9 shows that the rms roughness varied in the narrow range of 0.1-0.2 nm with the Ar gas flow rate. This shows a marginal effect of the Ar gas flow rate on the *a*-C film surface roughness.

## IV CONCLUSIONST

The effect of low-pressure Ar rf discharge on the growth of rf sputtered *a*-C films was investigated experimentally. It was found that the film thickness was a linear function of the product of the sputtering rate and deposition time. The effects of resputtering of carbon materials from the growing film surface by impinging $Ar^+$ and scattering during carbon atom transport through the plasma space between the target and the substrate on the film thickness were shown to be secondary. The principal factors affecting the film surface roughness are the film growth rate and the intensity of the $Ar^+$ bombardment. In the absence of energetic ion bombardment, the faster film growth the rougher the film surface. However, in the presence of energetic ion bombardment on the growing film surface, the *a*-C film surface roughness is controlled by the intensity of ion bombardment. Energetic particle bombardment on the growing film surface at ~210 eV enhanced carbon atom random motion at the surface, and promoted the growth of the smoothest *a*-C film. However, for ion bombardment energy above ~210 eV, the surface roughness increased due to the combined effects of increases resputtering and, especially, high irradiation damage.

## ACKNOWLEDGEMENTS

This research was supported by the National Science Foundation (Grant No. CMS-9734907) and the Computer Mechanics Laboratory at the University of California at Berkeley.

## REFERENCES

Tsai, H. and Bogy, D. B., Characterization of diamondlike carbon films and their application as a overcoats on thin film media for magnetic recording, *J. Vac. Sci. Technol. A* ***5***, 3287 (1987).

Lifshitz, Y., in *The Physics of Diamond*, edited by Paoletti and Tucciarone (IOS, Amsterdam, Netherlands, 1997), pp. 209-235.

Robertson, J., Diamond-like amorphous carbon, *Mater. Sci. Eng.* ***R37***, 129 (2002).

Durand, H. -A, Sekine, K., Etoh, K., Ito, K and Kataoka, I., Dynamic behavior of carbon ultrathin film formation, *J. Appl. Phys.* ***84***, 2591 (1998).

Logothetidis, S. and Stergioudis, G., Studies of density and surface roughness of ultrathin amorphous carbon films with regards to thickness with x-ray reflectometry and spectroscopic ellipsometry, Appl. Phys. Lett. **71**, 2463 (1997).

Schwan, J., Ulrich, S., Theel, T., Roth, H., Ehrhardt, H., Becker, P. and Silva, S. R. P., Stress-induced formation of high-density amorphous carbon thin films, *J. Appl. Phys.* ***82***, 6024 (1997).

Windischmann, H., Intrinsic stress in sputter-deposited thin films, *Crit. Rev. Solid State Mater. Sci.* ***17***, 547 (1992).

Davis, C. A., A simple model for the formation of compressive stress in thin films by ion bombardment, *Thin Solid Films* ***226***, 30 (1993).

Sigmund, P., Theory of sputtering. I. Sputtering yield of amorphous and polycrystalline targets, *Phys. Rev.****184***, 383 (1969).

Matsunami, N, Yamamura, Y., Itikawa, Y., Itoh, N., Kazumata, Y., Miyagawa, S., Morita, K., Shimizu, R. and Tawara, H., Energy dependence of the ion-induced sputtering yields of monatomic solids, *Atomic Data and Nuclear Data Tables* ***31*** (no. 1), 1 (1984).

Lieberman, M. A. and Lichtenberg, A. J., *Principles of Plasma Discharges and Materials Processing* (John Wiley & Sons, Inc., New York, 1994).

Table 1 Effect of absorbed rf power on *a*-C film thickness and surface roughness*

| Absorbed rf power (W) | Impinging flux ($\times 10^{15}$ ions/s·cm$^2$) | $Ar^+$ kinetic energy on target (eV) | $Ar^+$ kinetic energy on substrate (eV) | Thickness (nm) | Surface rms roughness (nm) |
|---|---|---|---|---|---|
| 172 | 4.61 | 509 | 210 | 5.6 | ___ |
| 285 | 5.43 | 800 | 210 | 10.9 | 0.09 ± 0.01 |
| 388 | 6.12 | 1010 | 210 | 15.6 | ___ |
| 500 | 6.78 | 1210 | 210 | 18.9 | 0.09 ± 0.01 |
| 600 | 7.04 | 1350 | 210 | 23.1 | 0.15 ± 0.01 |
| 739 | 7.99 | 1570 | 210 | 28.7 | 0.12 ± 0.01 |
| 298.5 | 5.16 | 1005 | 10 | 14.6 | 0.32 ± 0.07 |
| 401 | 5.89 | 1300 | 10 | 19.1 | 0.46 ± 0.04 |
| 496.5 | 6.73 | 1410 | 10 | 23.2 | 0.74 ± 0.06 |
| 595 | 7.30 | 1560 | 10 | 27.1 | 0.97 ± 0.11 |
| 741.5 | 8.08 | 1755 | 10 | 34.1 | 1.13 ± 0.14 |

* Deposition time = 3 min; Working pressure = 3 mTorr; Ar gas flow rate = 20 sccm.

Table 2 Effect of substrate bias on *a*-C film thickness and surface roughness*

| Substrate bias voltage (V) | Absorbed rf power (W) | Impinging flux ($\times 10^{15}$ ions/s·cm$^2$) | $Ar^+$ kinetic energy on target (eV) | Thickness (nm) | Surface rms roughness (nm) |
|---|---|---|---|---|---|
| 0 | 741.5 | 8.08 | 1755 | 34.1 | $1.13 \pm 0.14$ |
| -50 | 746.5 | 8.22 | 1695 | 32.2 | $0.60 \pm 0.04$ |
| -100 | 747.5 | 8.10 | 1640 | 30.8 | ___ |
| -150 | 744.5 | 8.13 | 1610 | 29.6 | $0.21 \pm 0.02$ |
| -200 | 739 | 7.99 | 1570 | 28.7 | $0.12 \pm 0.01$ |
| -300 | 715 | 8.26 | 1355 | 25.4 | $0.36 \pm 0.07$ |
| -400 | 675 | 8.44 | 1130 | ___ | $0.35 \pm 0.07$ |
| -500 | 672 | 8.56 | 1000 | ___ | $0.21 \pm 0.02$ |

*Deposition time = 3 min; Working pressure = 3 mTorr; Ar gas flow rate = 20 sccm.

Table 3 Effect of deposition time on *a*-C film thickness*

| Deposition Time (min) | Absorbed rf Power (W) | Impinging flux ($\times 10^{15}$ ions/s·cm$^2$) | $Ar^+$ kinetic energy on target (eV) | Thickness (nm) | Surface rms roughness (nm) |
|---|---|---|---|---|---|
| 3 | 739 | 7.99 | 1570 | 28.7 | 0.12 |
| 5 | 749 | 8.21 | 1545 | 46 | ___ |
| 7 | 746 | 8.19 | 1543 | 67 | ___ |
| 9 | 746 | 8.11 | 1560 | 85 | ___ |
| 11 | 747 | 8.12 | 1560 | 100 | ___ |

* Substrate bias voltage = -200 V; Working pressure = 3 mTorr;

Ar gas flow rate = 20 sccm.

**LIST OF FIGURES**

Figure 8 Effect of forward rf power on *a*-C film surface roughness for substrate bias voltage equal to -200 W and 0 V, working pressure of 3 mTorr, Ar gas flow rate of 20 sccm, and deposition time of 3 min.

Figure 9 Effect of Ar gas flow rate on *a*-C film surface roughness for forwarded rf power of 750 W, substrate bias voltage of -200 W, working pressure of 3 mTorr, and deposition time of 3 min.

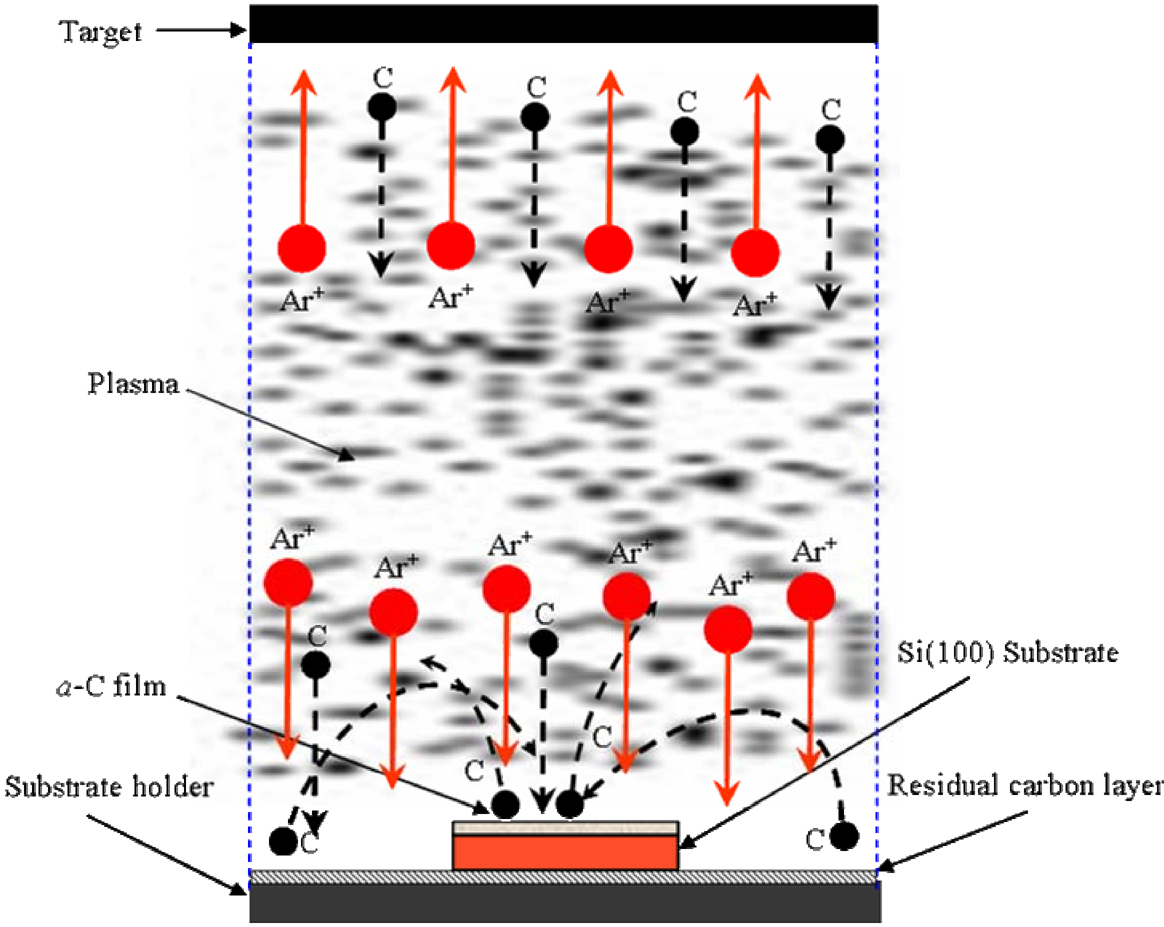
Target
C
C
C
C
Ar+
Ar+
Ar+
Ar+
Plasma
Ar+
Ar+
Ar+
Ar+
Ar+
Ar+
C
C
C
C
C
C
a-C film
Si(100) Substrate
Substrate holder
Residual carbon layer

Figure 1

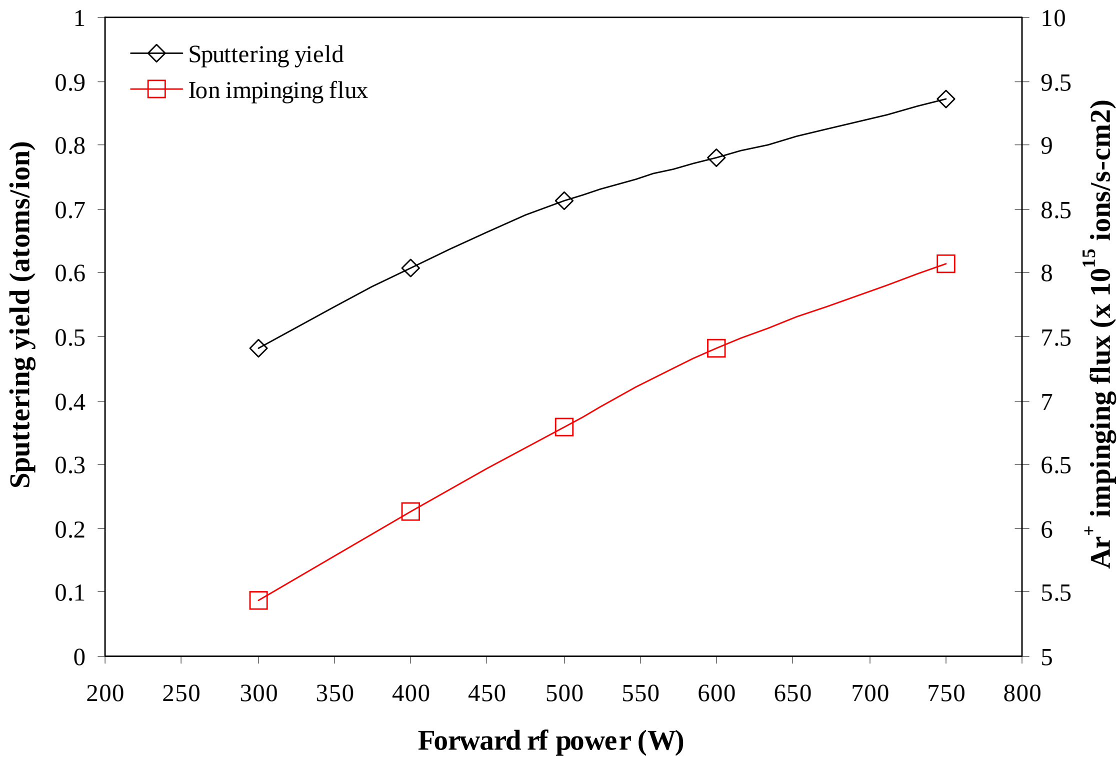

Sputtering yield
Ion impinging flux
Sputtering yield (atoms/ion)
Ar+ impinging flux (x 10^15 ions/s-cm2)
Forward rf power (W)
1
0.9
0.8
0.7
0.6
0.5
0.4
0.3
0.2
0.1
0
10
9.5
9
8.5
8
7.5
7
6.5
6
5.5
5
200
250
300
350
400
450
500
550
600
650
700
750
800


Figure 2

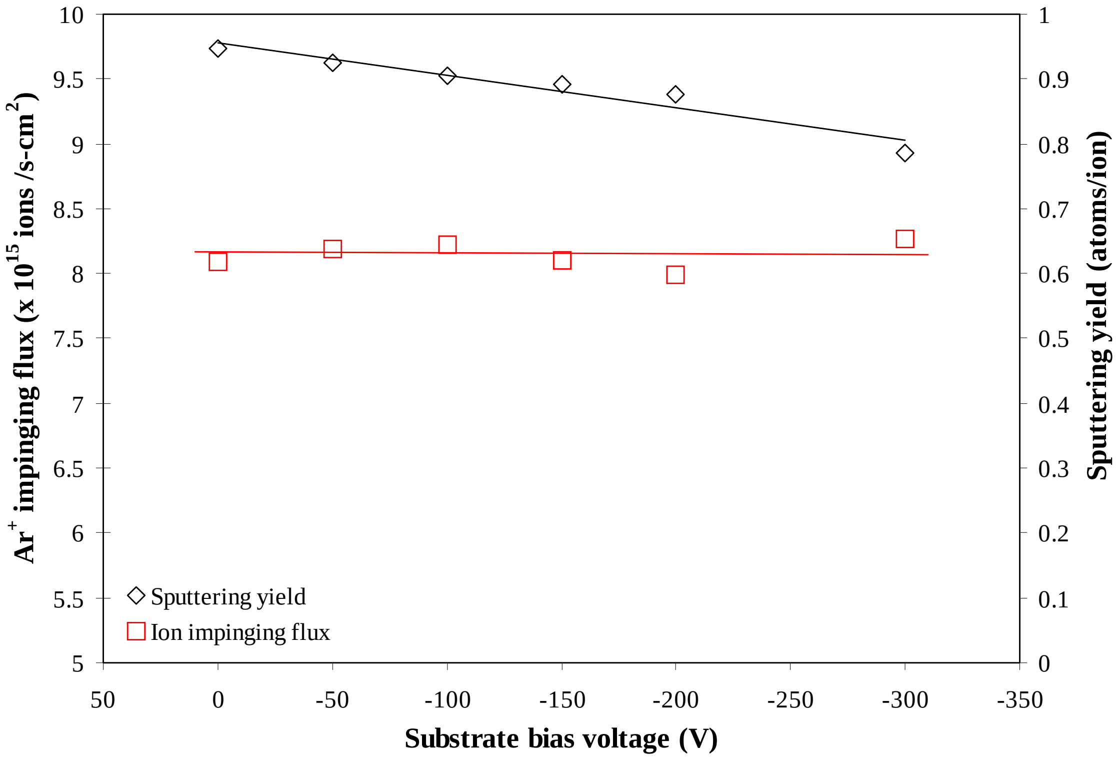

10
9.5
9
8.5
8
7.5
7
6.5
6
5.5
5
1
0.9
0.8
0.7
0.6
0.5
0.4
0.3
0.2
0.1
0
Ar+ impinging flux (x 10^15 ions /s-cm^2)
Sputtering yield (atoms/ion)
Sputtering yield
Ion impinging flux
50
0
-50
-100
-150
-200
-250
-300
-350
Substrate bias voltage (V)


Figure 3

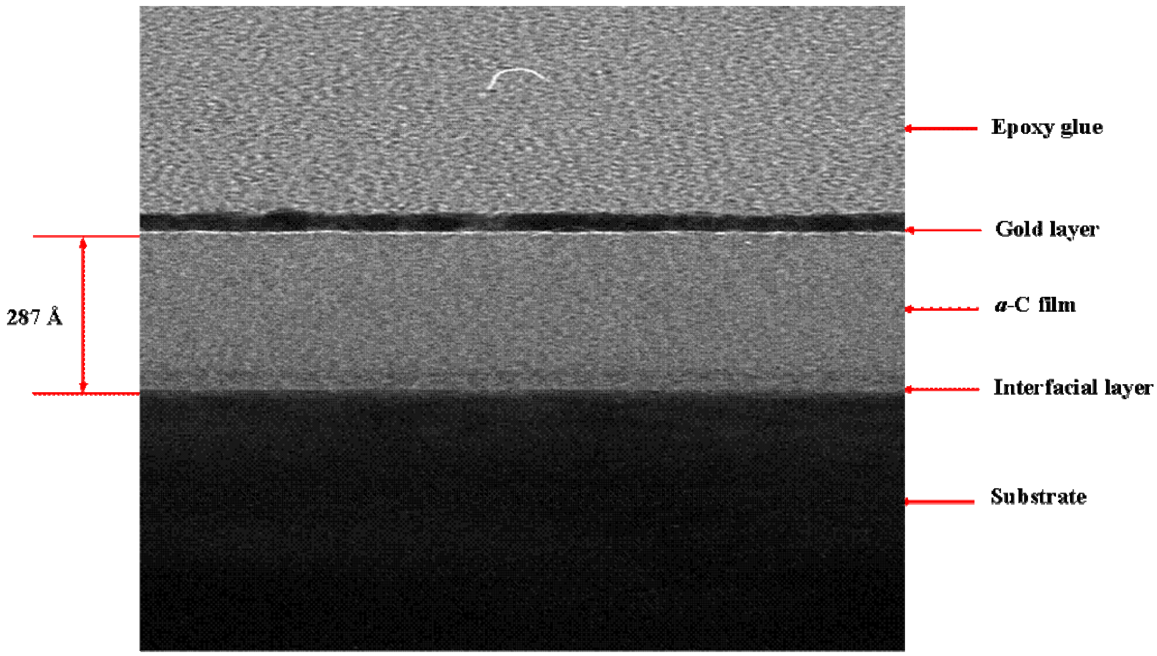
Epoxy glue
Gold layer
*a*-C film
Interfacial layer
Substrate
287 Å

Figure 4

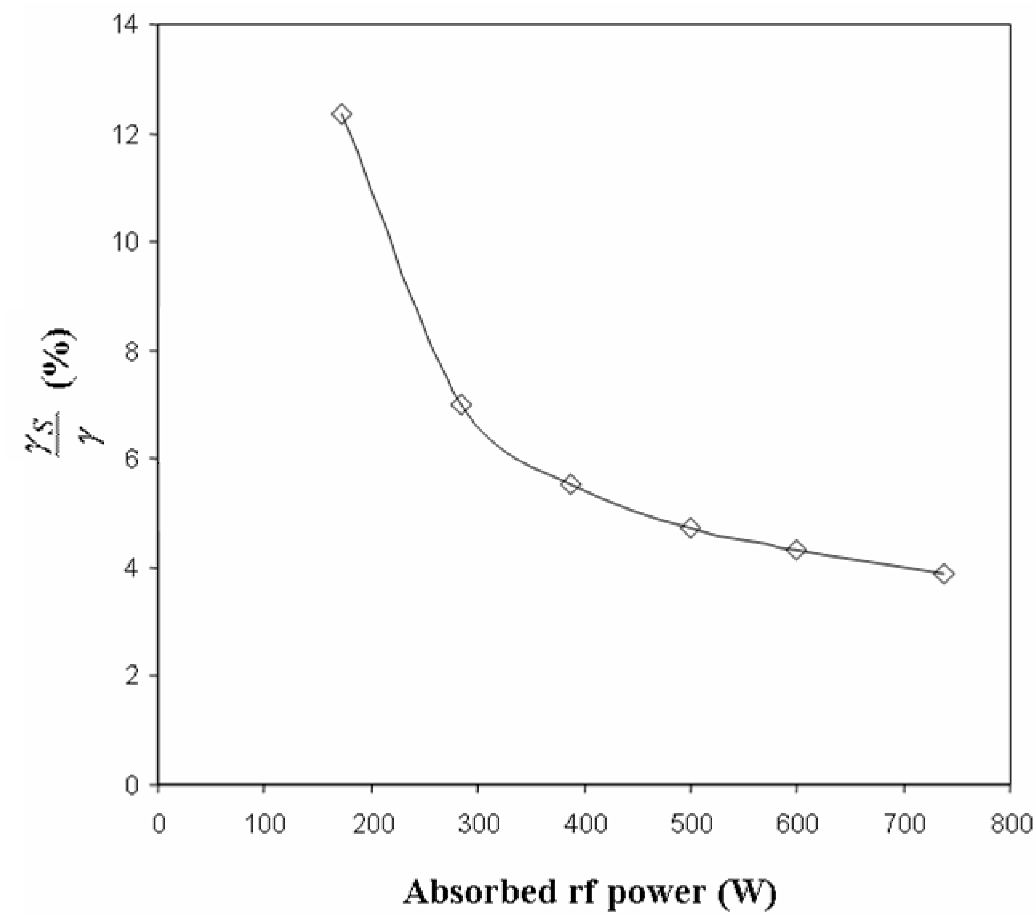

14
12
10
8
6
4
2
0
$\frac{\gamma_S}{\gamma}$ (%)
0
100
200
300
400
500
600
700
800
Absorbed rf power (W)


Figure 5

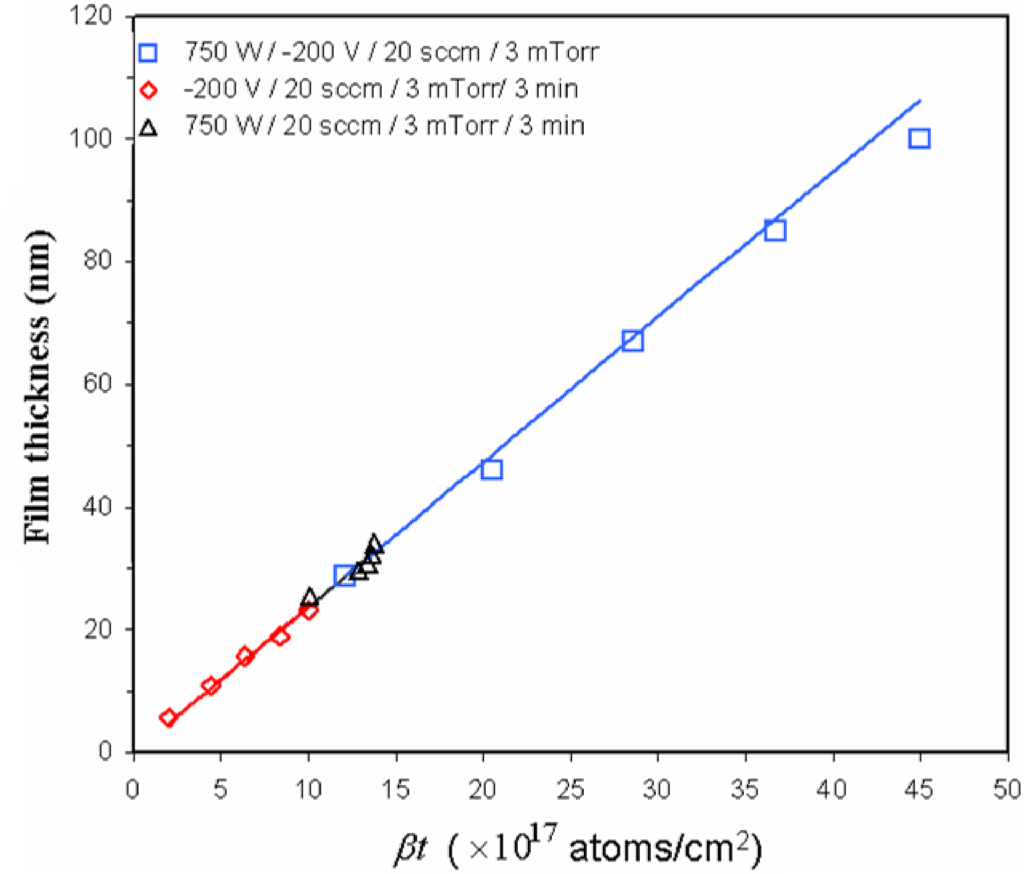
750 W / -200 V / 20 sccm / 3 mTorr
-200 V / 20 sccm / 3 mTorr/ 3 min
750 W / 20 sccm / 3 mTorr / 3 min
Film thickness (nm)
βt (×10^17 atoms/cm^2)
0
20
40
60
80
100
120
0
5
10
15
20
25
30
35
40
45
50

Figure 6

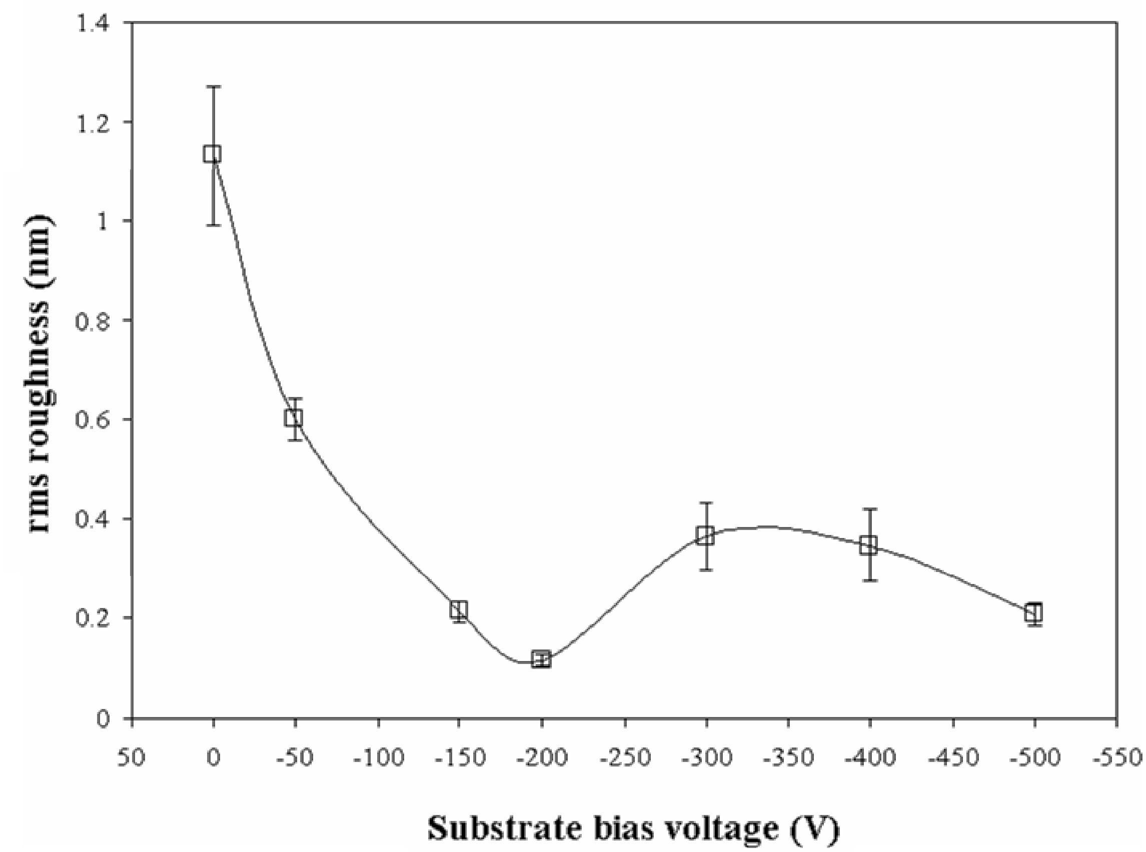
rms roughness (nm)
1.4
1.2
1
0.8
0.6
0.4
0.2
0
50
0
-50
-100
-150
-200
-250
-300
-350
-400
-450
-500
-550
Substrate bias voltage (V)

Figure 7

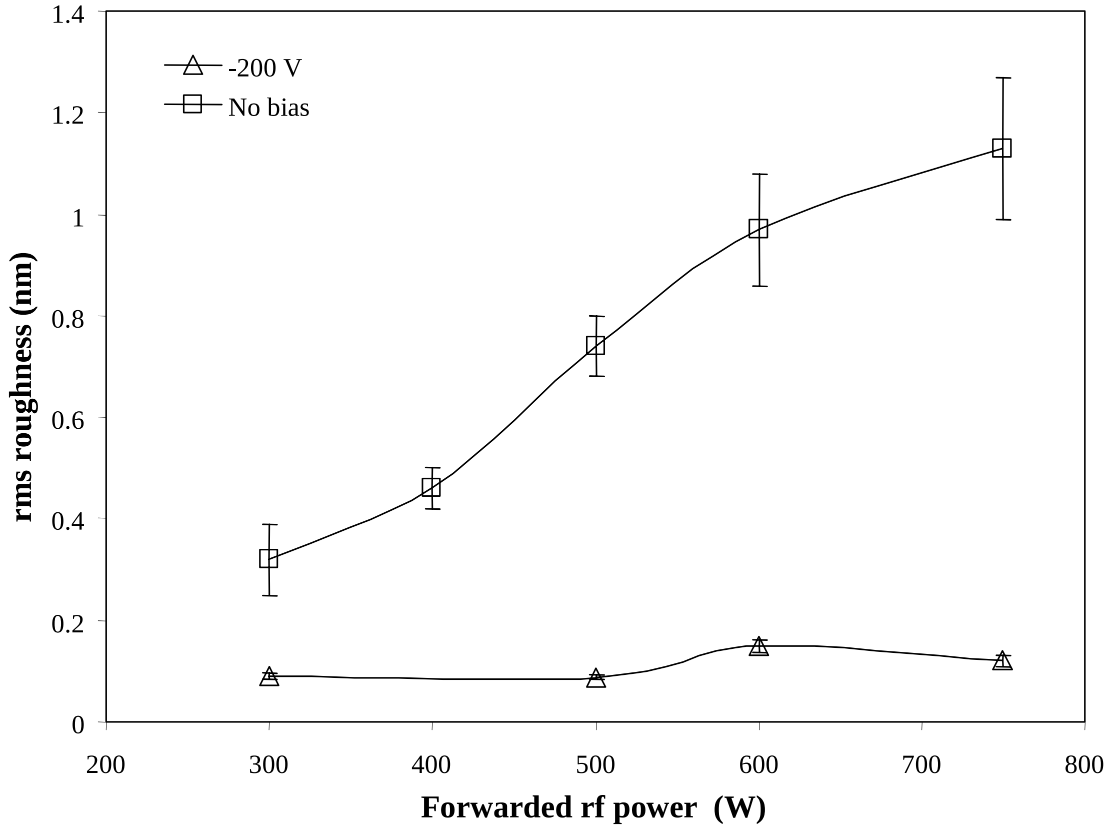
1.4
1.2
1
0.8
0.6
0.4
0.2
0
200
300
400
500
600
700
800
-200 V
No bias
rms roughness (nm)
Forwarded rf power (W)

Figure 8

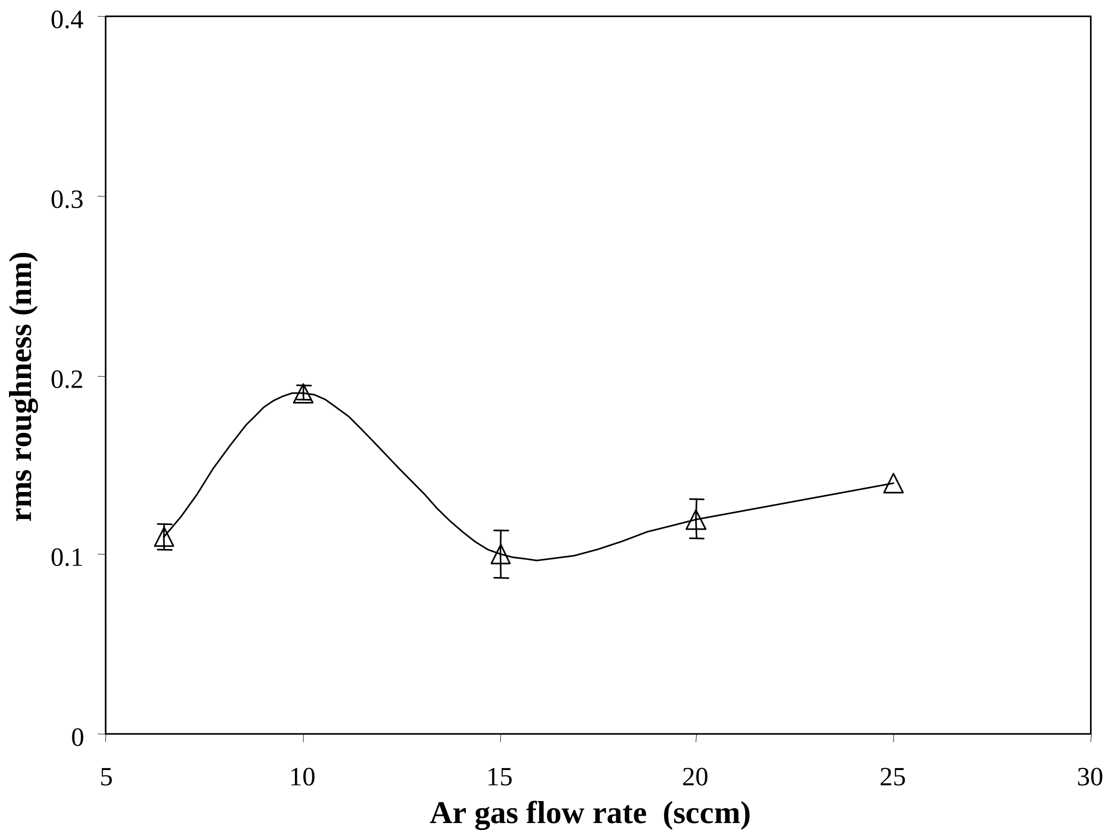

0.4
0.3
0.2
0.1
0
rms roughness (nm)
5
10
15
20
25
30
Ar gas flow rate (sccm)


Figure 9